

Dependence on volume of the phonon frequencies and the ir effective charges of several III-V semiconductors

J. A. Sanjurjo,* E. López-Cruz,† P. Vogl,‡ and M. Cardona
*Max-Planck-Institut für Festkörperforschung, Heisenbergstrasse 1,
 7000 Stuttgart 80, Federal Republic of Germany*

(Received 23 June 1983)

The mode Grüneisen parameters of the LO and TO Raman phonons of AlN, BN, and BP, and the dependence of e_T^* on lattice constant have been measured by Raman scattering in a diamond anvil cell. The results for e_T^* are interpreted by means of pseudopotential calculations of e_T^* versus lattice constant.

I. INTRODUCTION

The advent of the diamond anvil cell has made possible the accurate determination of mode Grüneisen parameters of phonons in semiconductors by means of Raman spectroscopy.¹⁻³ Of particular interest has also been the volume dependence of the transverse effective charge which can be related to the dependence of the ionicity of the chemical bond on bond length.^{3,4} The volume dependence of e_T^* has been measured for several III-V (Refs. 1-3) and II-VI (Ref. 5) compounds (GaAs, GaP, InP, ZnS, ZnSe, and ZnTe) and for zinc-blende-type (*a-*) SiC.⁶ In all these cases, with the exception of SiC, $|e_T^*|$ and thus the ionicity has been found to decrease with decreasing bond length. For SiC the opposite occurs. A semi-quantitative interpretation of these results by means of a pseudopotential band-structure calculation of e_T^* has been made.^{3,6} The anomalous sign of the derivative of $|e_T^*|$ with respect to the bond length results from the strong difference in the pseudopotentials of C and Si for small wave vectors, which in turn is related to the lack of *p* electrons in the core of the carbon atoms.

In this paper we present similar data for the more exotic large-band-gap III-V compounds BN, AlN, and BP. Reliable values of the effective charges of these materials are given. The mode Grüneisen parameters γ_{LO} and γ_{TO} are similar to those found for the equivalent phonons of similar semiconductors (γ between 1 and 1.6 with $\gamma_{TO} > \gamma_{LO}$). The dependence of e_T^* on bond length for AlN and BP might have been similar to that of SiC according to Periodic Table systematics. We found, however, that in all three cases $|e_T^*|$ decreased with decreasing bond length. These results agree qualitatively with pseudopotential calculations in spite of the difficulties encountered with the pseudopotentials of the first row of the Periodic Table.

II. EXPERIMENTAL DETAILS

The AlN samples used in the high-pressure measurements were prepared by polishing down to a thickness of 30 μm a film grown at the IBM Yorktown Heights Research Center on a sapphire substrate. A platelet of BP was polished to a thickness of 30 μm . These thin platelets

were broken into small pieces and in each case one of them, suitable to fit into the 200- μm hole of the pressure cell gasket, was chosen under the microscope. For samples of BN, several small crystallites approximately 200 μm in diameter were glued together and polished down to a 20 μm thickness. The final samples were of the appropriate size to fit into the hole of the pressure-cell gasket.

A gasketed diamond anvil cell similar to that reported by Syassen and Holzapfel⁷ was employed for the Raman measurements. A 4:1 methanol-ethanol mixture served as the pressure medium; the fluorescence of a tiny ruby chip placed near the samples was used for the pressure calibration.⁸ The Raman spectra were excited in backscattering geometry with the 5145-Å (2.41-eV) line of an Ar⁺-ion gas laser. The scattered light was analyzed with a Spex 1401 double monochromator and detected with a RCA C31034 photomultiplier in the photon counting mode. All measurements were carried out at room temperature.

III. RESULTS

Figure 1 shows typical first-order Raman spectra of the TO and LO phonons in zinc-blende-type BP and BN, and for the A_1 and E_1 TO and LO phonons in wurtzite AlN for various pressures. The frequencies of the TO and LO modes for zero pressure agree with values reported by other authors, with the exception of the TO phonon in BP.^{9,10} In all cases the LO(Γ)-TO(Γ) splitting decreases with increasing pressures. Figures 2-4 display the peak position of the LO and TO Raman lines as a function of pressure (bottom horizontal scale) and the relative lattice compression $-\Delta a/a_0$ (top horizontal scale) for BP, BN, and AlN, respectively. The Raman peaks show, within the experimental error, a linear dependence with pressure in the measurement range. The solid lines in Figs. 2-4 are the least-squares fits to the data using the equations

$$\omega_{LO}^{BP} = (828.9 \pm 0.6) + (4.89 \pm 0.07)p, \quad (1)$$

$$\omega_{TO}^{BP} = (799 \pm 1) + (5.48 \pm 0.08)p,$$

$$\omega_{LO}^{BN} = (1305 \pm 1) + (3.45 \pm 0.07)p, \quad (2)$$

$$\omega_{TO}^{BN} = (1054.7 \pm 0.6) + (3.39 \pm 0.08)p,$$

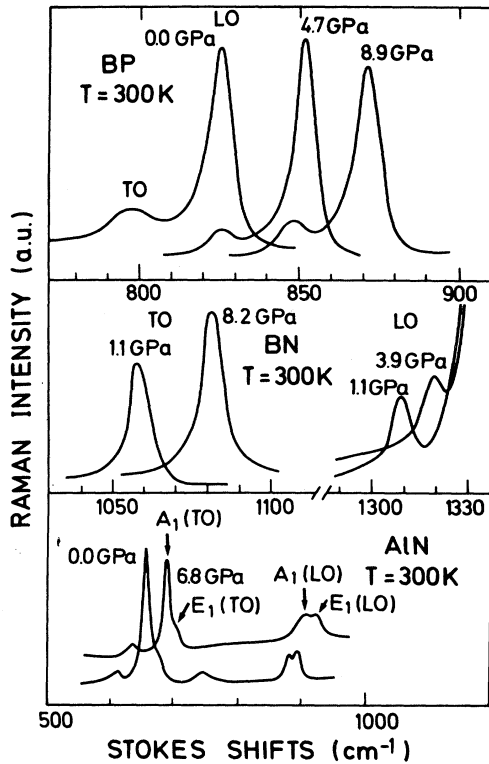


FIG. 1. First-order Raman spectra of BP, BN, and AlN obtained at room temperature under different hydrostatic pressures.

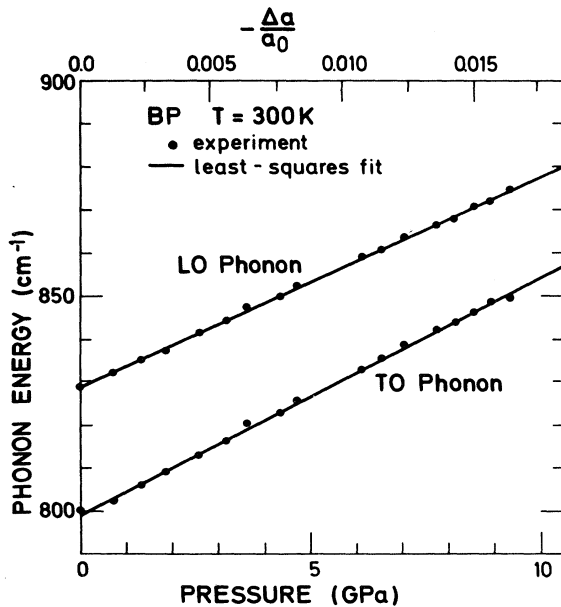


FIG. 2. Dependence of the LO(Γ) and TO(Γ) phonon frequencies of BP with pressure (lower scale) and relative lattice compression (upper scale). Solid lines are least-squares fits to the experimental points with Eq. (1).

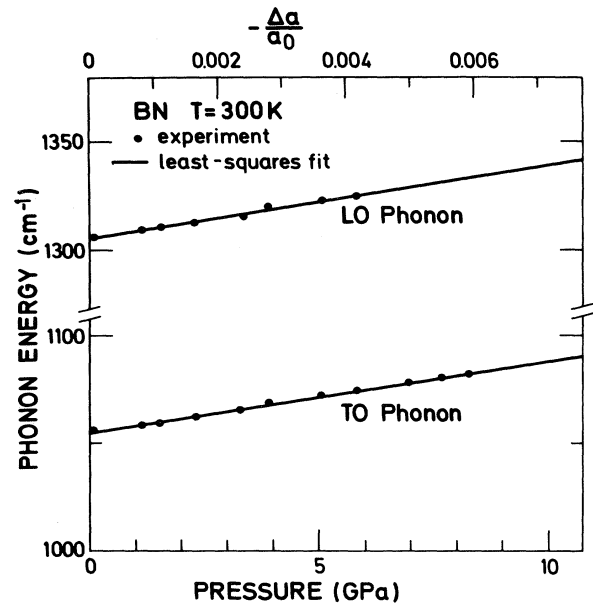


FIG. 3. Dependence of the LO(Γ) and TO(Γ) phonon frequencies of BN with pressure (lower scale) and relative lattice compression (upper scale). Solid lines are least-squares fits to the experimental points with Eq. (2).

$$\omega_{\text{LO}}^{\text{AlN}}(E_1) = (895 \pm 2) + (4.0 \pm 0.2)p,$$

$$\omega_{\text{TO}}^{\text{AlN}}(E_1) = (671.6 \pm 0.8) + (4.84 \pm 0.09)p, \quad (3)$$

$$\omega_{\text{LO}}^{\text{AlN}}(A_1) = (888 \pm 2) + (3.8 \pm 0.2)p,$$

$$\omega_{\text{TO}}^{\text{AlN}}(A_1) = (659.3 \pm 0.6) + (4.97 \pm 0.06)p,$$

with ω_{TO} and ω_{LO} in cm^{-1} and p in GPa. In hexagonal AlN the A_1 and E_1 anisotropy, as can be seen in Fig. 4, is small. This consideration enables us to define an effective average value for the longitudinal frequency $\bar{\omega}_{\text{LO}}^2 = [\omega_{\text{LO}}^2(A_1) + 2\omega_{\text{LO}}^2(E_1)]/3$ and a similar expression for $\bar{\omega}_{\text{TO}}^2$.¹¹ The pressure dependence found for these average frequencies is

$$\bar{\omega}_{\text{LO}}^{\text{AlN}} = (893 \pm 2) + (3.9 \pm 0.2)p, \quad (4)$$

$$\bar{\omega}_{\text{TO}}^{\text{AlN}} = (667.5 \pm 0.7) + (4.88 \pm 0.08)p.$$

In Table I we list the relevant parameters used in this work, i.e., the zero-pressure lattice constant (a_0), bulk modulus (B_0), and the high-frequency dielectric constant (ϵ_∞), as well as the optical frequencies just obtained.

The mode Grüneisen parameters γ_i are defined as

$$\gamma_i = -\frac{\partial \ln \omega_i}{\partial \ln V} = \frac{B_0}{\omega_i} \frac{d\omega_i}{dp}, \quad (5)$$

where the ω_i 's are given phonon modes [LO(Γ) and TO(Γ) in our case]. In order to evaluate the γ_i 's we need the bulk moduli B_0 . Unfortunately, only few data are available for the elastic properties of the materials at hand. With the exception of BP, for which the elastic constants are known, the bulk moduli were estimated by using

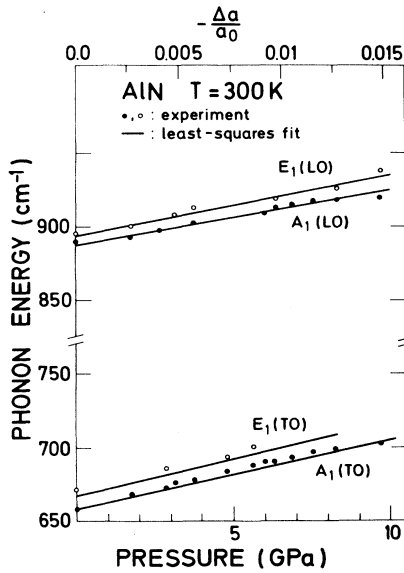


FIG. 4. Dependence of the LO(Γ) and TO(Γ) phonon frequencies of AlN with pressure (lower scale) and relative lattice compression (upper scale). Solid lines are least-squares fits to the experimental points with Eq. (3).

empirical relations for the elastic constants.¹³ They are listed in Table I together with other parameters needed for the discussion. For AlN we used the relation $a_0^3 = \sqrt{3}a^2c$ to define an effective cubic lattice constant a_0 from the hexagonal constants a and c of this material. The values of γ_{TO} and γ_{LO} found from Eqs. (1)–(4) with the B 's of Table I are given in Table II. They are similar to the values found for other diamond and zinc-blende-type semiconductors.^{1–3,6} In zinc-blende-type semiconductors the Born transverse effective charge is related to the splitting of the long-wavelength LO and TO phonon modes⁴

$$e_T^{*2} = \frac{\epsilon_\infty a_0^3 \mu}{16\pi} (\omega_{LO}^2 - \omega_{TO}^2). \quad (6)$$

In Eq. (5) μ is the reduced mass of the two-component atoms ($\mu^{-1} = m_A^{-1} + m_B^{-1}$), a_0 the cubic lattice constant, and ϵ_∞ the infrared dielectric constant. To calculate the

dependence of e_T^* on volume, we encounter the difficulty that the volume dependence of ϵ_∞ is not known experimentally. We have taken for all three compounds the same value as for SiC,⁶ that is, $d \ln \epsilon_\infty / d \ln a_0 \approx 1.8$. This step sounds justified in view of the discussion given in Ref. 14. With the use of the data of Figs. 2–4, Eq. (5), and the data of Table I, we obtain the dependence of e_T^* on the lattice constant displayed in Fig. 5. In AlN and BP, e_T^* decreases clearly with increasing pressure, while BN shows a very small decrease with pressure. The solid lines in Fig. 5 are the least-squares fits to the data. The values of e_T^* at zero pressure, as well as $\partial e_T^* / \partial \ln a$ and $\gamma e_T^* = \partial \ln e_T^* / \partial \ln V$ obtained from the above fit, are listed in Table II. For comparison we also show in Table II previous results found for SiC,⁶ InP,³ and GaAs.¹⁵

IV. DISCUSSION

Two different types of approaches can be used to calculate e_T^* and its volume dependence. The first is based on semiempirical models of the tetrahedral bond. With this model⁴ we find

$$e_T^* = -\Delta Z + \frac{30}{3}\alpha_p - \frac{8}{3}\alpha_p^3, \quad (7)$$

where ΔZ is one-half the difference in core charges between the anion and the cation ($\Delta Z = 0, 1, 2$ for IV-IV, III-V, and II-VI compounds, respectively) and α_p is the polarity of the bond defined in Ref. 4. By choice of the sign e_T^* represents the charge of the cation. The dependence of the polarity on lattice constant is given by^{3,4}

$$\frac{\partial \alpha_p}{\partial \ln a_0} = 2\alpha_p(1 - \alpha_p^2), \quad (8)$$

with Eqs. (7) and (8) we obtain the values listed in columns 6 and 9 of Table II. Another approach is to use the microscopic pseudopotential expression for e_T^* in the way followed recently for InP and SiC.^{3,6} The results of this full pseudopotential calculation are listed in columns 5 and 8 of Table II.

The theoretical calculations of e_T^* are based on the pseudopotential expression¹⁶

$$e_T^* = -\Delta Z + \frac{2}{N} \sum_{\vec{G} \neq 0} \sum_n^{\text{VB}} \sum_{n'}^{\text{CB}} \sum_{\vec{k}} \frac{\langle n, \vec{k} | p_x | n', \vec{k} \rangle \langle n', \vec{k} | e^{i\vec{G} \cdot \vec{\tau}} | n, \vec{k} \rangle}{(E_{nk} - E_{n'k})^2} G_x [i v_s(\vec{G}) \sin \vec{G} \cdot \vec{\tau} - v_a(\vec{G}) \cos \vec{G} \cdot \vec{\tau}]. \quad (9)$$

TABLE I. Relevant parameters for AlN, BN, and BP used in this work and measured zero-pressure zone-center phonons.

	$\omega_{TO}(p=0)$ cm ⁻¹	$\omega_{LO}(p=0)$ cm ⁻¹	a_0 Å	B_0 GPa	ϵ_∞
AlN	667.5(7)	893(2)	4.37(3) ^a	218(20) ^b	4.76(8) ^a
BN	1054.7(6)	1305(1)	3.6155(2) ^a	465(50) ^b	4.50(2) ^a
BP	799(1)	828.9(6)	4.5383(4) ^a	190(15) ^c	9.61(2) ^a

^aLandolt-Börnstein Tables, edited by O. Madelung (Springer, Berlin, 1982), Vol. III, 17a.

^bInterpolated using empirical relations for the elastic constants (Ref. 13).

^cReference 12.

TABLE II. Mode Grüneisen parameters of the zone-center phonons, transverse effective charge, and its variation with lattice constant as measured experimentally and as calculated with various pseudopotential approaches for various III-V compounds and SiC.

Compound	γ_{TO} (Expt.)	γ_{LO} (Expt.)	e_T^*			$\partial e_T^* / \partial \ln a_0$			$\gamma_{e_T^*}$ experimental
			Expt. (absolute value)	Full pseudo- potential calculation	BOM Harrison	Expt.	Full pseudo- potential calculation	BOM Harrison ^a	
AlN	1.6(2)	1.0(1)	2.57(3)	2.91	2.36	5(2)	1	3.06	-0.65
BN	1.5(1)	1.2(1)	1.984(5)	2.78	1.17	1.01(7)	4	3.45	-0.17
BP	1.3(1)	1.12(9)	1.34(1)	-1.38	0.31	10(2)	+2	2.44	-2.49
SiC ^b	1.56(1)	1.55(1)	2.697(4)	2.81	1.69	-5.4(1)	-14.1	2.97	0.67
InP ^c	1.44(2)	1.24(2)	2.54	1.81	2.35	4.5	8.5	3.06	-0.59
GaAs ^{c,d}	1.39(2)	1.23(2)	2.18	1.71	1.86	4.4	8.3 ^e	3.59	-0.67
GaP	1.09	0.95	2.04 ^a	2.11 ^e	2.05	1.5 ^f	8.8	3.46	-0.5 ^f
						2.6 ^g			-0.85 ^g

^aReference 4.

^bReference 6.

^cReference 3.

^dReference 15.

^eReference 16.

^fReference 2.

^gG. A. Samara, Phys. Rev. B **27**, 3494 (1983).

This expression follows from a calculation of the macroscopic dipole moment which is induced by a small ionic displacement at zero macroscopic electric field. Equation (9) is derived in the framework of linear-response theory with the Hartree approximation and the method of long waves. The single-particle Bloch states $|n, \vec{k}\rangle$ and the energies $E_{n, \vec{k}}$ of the electrons are calculated with the local, empirical pseudopotential method. N denotes the number of unit cells, the \vec{G} 's are the reciprocal-lattice vectors, \vec{p} is

the momentum operator, and $\vec{\tau} = (a/8)(1,1,1)$. The first term in Eq. (9) arises from the bare core charges. The $v_s(\vec{G})$ and $v_a(\vec{G})$ are the symmetric and antisymmetric combinations of the screened atomic pseudopotential form factors. For AlP,¹⁷ GaN,¹⁸ AlN,¹⁸ and BP,¹⁹ we used previously published empirical form factors. For BN, the B and N form factors normalized to a fixed volume were taken from the interpolated BP (Ref. 19) and AlN (Ref. 18) pseudopotentials, respectively, rather than directly from Ref. 19, in order to maintain the transferability of the pseudopotentials. This is essential for the conceptual validity of the empirical pseudopotential method. It should be mentioned that the neglect of nonlocality (angular momentum dependence) of the carbon-row atomic pseudopotentials is actually quite a crude approximation due to the absence of p electrons in the core.²⁰

The pseudopotential form factors which we used in this paper are tabulated in Table III. Eighty-nine plane waves and ten special \vec{k} points were included in the numerical calculation of Eq. (9). To calculate the pressure dependence of e_T^* , the atomic form factors are needed at the pressure-shifted \vec{G} 's and have to be renormalized to the compressed unit-cell volume. We have truncated the perfect-crystal form factors beyond $q_{cut} = 3k_F$ and then interpolated them by a cubic spline in order to obtain these form factors. In addition, the rigid-ion approximation was adopted, where the dominant dependence of $v(\vec{G})$ on the lattice constant arises solely from the normalizing cell volume Ω , $v(\vec{G}) \propto \Omega^{-1}$.²⁰

The results of the pseudopotential calculations are summarized in Table III. The theoretical values for e_T^* agree well with the experimental values while the pressure coefficients of e_T^* generally agree only qualitatively with the data. However, the calculations in all cases reproduce the experimentally found sign of $\partial |e_T^*| / \partial p$. This sign has an interesting physical origin which will be discussed now.

A simple and physically illuminating expression for e_T^*

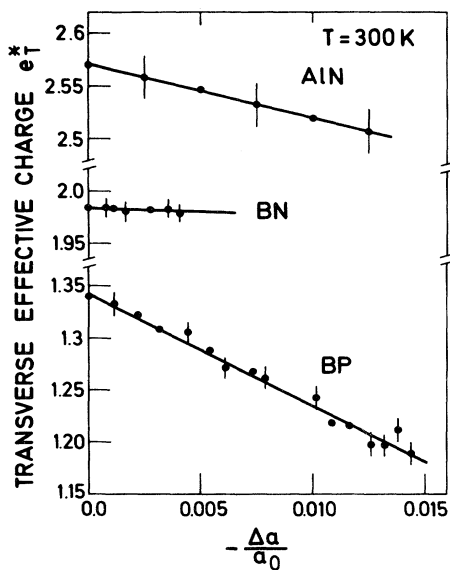


FIG. 5. Dependence on lattice compression of the transverse effective charge for BP, BN, and AlN. Points were obtained from the measured pressure dependence of the LO and TO phonons of Figs. 2-4 using Eq. (6). Solid lines are least-squares fits to the experimental points.

TABLE III. Pseudopotential form factors (in Ry) for various III-V compounds used to calculate e_T^* with Eq. (9).

	BN	BP	AlN	GaN	AlP
$v_s(3)$	-0.585	-0.373	-0.310	-0.340	-0.210
$v_s(4)$	-0.320	-0.260	-0.221	-0.229	-0.130
$v_s(8)$	0.155	-0.085	0.011	0.018	0.040
$v_s(11)$	0.070	0.099	0.070	0.070	0.080
$v_s(12)$	0.013	0.091	0.092	0.069	0.076
$v_a(3)$	0.265	0.010	0.280	0.270	0.130
$v_a(4)$	0.320	0.023	0.275	0.243	0.080
$v_a(8)$	0.015	0.038	0.119	0.132	0.023
$v_a(11)$	-0.050	0.034	-0.010	0.040	0.015
$v_a(12)$	-0.026	0.033	-0.032	0.018	0.012

can be obtained from Eq. (9) by neglecting all pseudopotential form factors but the dominating ones $v_s(3)$ and $v_a(3)$, with $|\vec{G}| = (2\pi/a)\sqrt{3}$. The Bloch states can then be evaluated explicitly and one finds¹⁶

$$e_T^* = -\Delta Z + \frac{8p_i}{1+p_i^2}, \quad (10)$$

$$p_i = -\frac{v_a(3)}{v_s(3)}.$$

The ratio p_i plays the role of a "polarity" [cf. Eq. (7)] and is defined in such a way that $0 < p_i < 1$ for most semiconductors (cf. Table III). Taking the derivative of Eq. (10) with respect to the lattice constant

$$\frac{\partial e_T^*}{\partial a} = 8 \frac{1-p_i^2}{(1+p_i^2)^2} \frac{\partial p_i}{\partial a}, \quad (11)$$

one sees that the sign of $\partial e_T^*/\partial a$ equals that of $\partial p_i/\partial a$, i.e., e_T^* will decrease with pressure if the polarity also decreases with pressure.

The pressure dependence of p_i follows the pressure dependence of the pseudopotentials. The origin of this dependence can be seen most clearly by considering model pseudopotentials rather than empirical form factors which qualitatively agree with one another.²⁰ The atomic form factors (A = anion, C = cation) $v_A(q)$, $v_C(q)$ behave like screened Coulomb potentials for $q \rightarrow 0$, $v_{A,C}(q) \rightarrow -4\pi Z_{A,C}/\epsilon(q)q^2$. For q of the order of the inverse core radius, $1/R^{\text{core}}$, on the other hand, the pseudopotentials tend to become small and to oscillate around zero. In a IV-IV compound, such as SiC, the form factors of Si and C approach each other for $q \rightarrow 0$, since $Z_{\text{Si}} = Z_{\text{C}} = 4$, but they differ considerably for large q since $R_{\text{C}}^{\text{core}} \ll R_{\text{Si}}^{\text{core}}$. The above behavior is displayed qualitatively in Fig. 6. As a consequence, the difference $v_a = (v_{\text{Si}} - v_{\text{C}})/2$ as well as the polarity p_i increase when τ 's are shifted to larger q , a fact which corresponds to increased pressure. Therefore, IV-IV compounds are predicted to have the effective charge increased with pressure, in agreement with experiment.⁶ In a typical III-V compound such as GaAs, on the other hand, the form factors differ for $q \rightarrow 0$ since $Z_{\text{Ga}} = 3$, $Z_{\text{As}} = 5$, but they become close for large q since these atoms have comparable core radii (see Fig. 6). As a consequence, most III-V com-

pounds and also II-VI compounds are expected to show a decreasing e_T^* with increasing pressure, again in agreement with experiment. Since e_T^* is a measure of ionicity ($e_T^* = 0$ in Si), one concludes that this ionicity decreases with pressure in GaAs but increases with pressure in SiC.

In this paper we have studied III-V compounds with group-III atoms from the carbon row of the Periodic Table which have very small core radii. In these cases, the pseudopotentials differ significantly for $q \rightarrow 0$ and for $q \sim 1/R^{\text{core}}$. From the previous discussions it is clear that these compounds therefore represent borderline cases between the "normal" ($\partial |e_T^*|/\partial a > 0$) and anomalous pressure dependence ($\partial |e_T^*|/\partial a < 0$) of e_T^* . While AlN and BN still behave like GaAs, BP is found theoretically to behave anomalously. As can be deduced from Table II, the polarity $p_i \simeq 0$ in BP, which implies the effective charge of B to be negative $e_T^* \simeq -1$, according to the analytical expression Eq. (10).

The full pseudopotential calculation gives $e_T^* = -1.38$ for BP. The pressure coefficient of p_i and e_T^* in BP is theoretically found to be anomalous, $\partial p_i/\partial a < 0$, as in SiC. Experimentally, only $|e_T^*|$ can be measured optically and since e_T^* itself is negative, one also obtains $\partial |e_T^*|/\partial a > 0$ for this material.

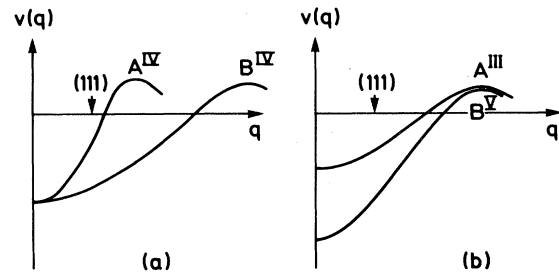


FIG. 6. Schematic drawing of screened atomic pseudopotential form factors $v(q)$ as a function of wave vector q for a typical IV-IV compound such as (a) SiC and for a typical III-V compound such as (b) GaAs. The approximate position of the first reciprocal-lattice vector is indicated by arrows. Under pressure the reciprocal-lattice vector increases. Correspondingly, the "ionicity" as measured by the difference of the A and B (111) pseudopotential form factors increases in a IV-IV compound but decreases in a III-V compound.

ACKNOWLEDGMENTS

The help of W. Dieterich and I. Stoll in loading the diamond cell is gratefully acknowledged. We would like to thank Dr. W. Wettling for making his elastic-constants data for BP available to us prior to publication, and Dr. J. Schneider for help in obtaining the BP and BN crystals used. The BP crystals were kindly supplied by Dr. T. Kimura, University of Electrocommunications, Tokyo and the BN crystals by deBeers Industrial Diamonds

Division, Shannon, Ireland. The AlN crystals were provided by Dr. R. F. Rutz (IBM Thomas J. Watson Research Center, Yorktown Heights) and Dr. R. Tsu (Energy Conversion Devices, Inc., Troy, MI) to whom thanks are also due. One of us (E.L.C.) acknowledges the financial support of Consejo Nacional de Ciencia y Tecnología (México). Partial support by the Fonds zur Förderung der wissenschaftlichen Forschung in Österreich, Projekt Nr. 4236, is also acknowledged.

*Instituto de Física Gleb Wataghin, Universidade Estadual de Campinas, 13100 Campinas, São Paulo, Brazil.

†Departamento de Física, Instituto de Ciencias, Universidad Autónoma de Puebla, Apartado J-48, CP-72570 Puebla, Pue, Mexico.

‡Institut für Theoretische Physik der Universität Graz, Universitätsplatz 5, A-8010 Graz, Austria.

¹B. A. Weinstein and G. Piermarini, Phys. Rev. B **12**, 1172 (1975).

²B. A. Weinstein and R. Zallen, in Topics in Applied Physics, edited by G. Güntherodt and M. Cardona (Springer, Heidelberg, in press).

³R. Trommer, H. Müller, M. Cardona, and P. Vogl, Phys. Rev. B **21**, 4869 (1980).

⁴W. A. Harrison, *Electronic Structure and the Properties of Solids* (Freeman, San Francisco, 1980).

⁵B. A. Weinstein, Solid State Commun. **12**, 473 (1973).

⁶D. Olego, M. Cardona, and P. Vogl, Phys. Rev. B **25**, 3878 (1982).

⁷K. Syassen and W. Holzapfel, Phys. Rev. B **18**, 5826 (1978).

⁸J. D. Barnett, S. Block, and G. J. Piermarini, Rev. Sci. Instrum. **44**, 1 (1973); G. J. Piermarini, S. Block, J. O. Barnett, and R. A. Forman, J. Appl. Phys. **46**, 2774 (1975).

⁹O. Brafman, G. Lengyel, S. S. Mitra, P. J. Gielisse, J. N. Plendl, and L. C. Mansur, Solid State Commun. **6**, 523

(1968).

¹⁰R. Tsu and R. F. Rutz, in *Proceedings of the Third International Conference on Light Scattering in Solids*, edited by M. Balkanski, R. C. C. Leite, and S. P. S. Porto (Flammarion, Paris, 1976), p. 393.

¹¹G. Lucovsky, R. M. Martin, and E. Burstein, Phys. Rev. B **4**, 1367 (1971).

¹²W. Wettling (private communication).

¹³E. F. Steigmeier, Appl. Phys. Lett. **3**, 6 (1963).

¹⁴M. Cardona, in *Atomic Structure and Optical Properties of Solids*, edited by E. Burstein (Academic, New York, 1972), p. 197.

¹⁵R. Trommer, E. Anastassakis, and M. Cardona, in *Light Scattering in Solids*, edited by M. Balkanski, R. C. C. Leite, and S. P. S. Porto (Flammarion, Paris, 1976), p. 396.

¹⁶P. Vogl, J. Phys. C **11**, 251 (1978).

¹⁷Y. F. Tsay, A. J. Corey, and S. S. Mitra, Phys. Rev. B **12**, 1354 (1975).

¹⁸S. Bloom, J. Phys. Chem. Solids **32**, 2027 (1971).

¹⁹L. A. Hemstreet, Jr. and C. Y. Fang, Phys. Rev. B **6**, 1464 (1972).

²⁰M. L. Cohen and V. Heine, in *Solid State Physics*, edited by H. Ehrenreich, F. Seitz, and D. Turnbull (Academic, New York, 1970), Vol. 24, p. 37.